Biogeosciences Discuss., 8, 2001–2033, 2011
www.biogeosciences-discuss.net/8/2001/2011/
doi:10.5194/bgd-8-2001-2011

Biogeosciences Discussions

Role of net radiation on energy balance closure in heterogeneous grasslands

C. Shao[1,2], J. Chen[1,2], L. Li[1], G. Tenney[2], W. Xu[1], and J. Xu[2]

[1]Key Laboratory of Vegetation and Environmental Change, Institute of Botany, Chinese Academy of Sciences, Beijing 100093, China
[2]Department of Environmental Sciences, University of Toledo, Toledo, OH 43606, USA

Received: 12 January 2011 – Accepted: 9 February 2011 – Published: 1 March 2011

Correspondence to: C. Shao (zkyscl@ibcas.ac.cn)

Published by Copernicus Publications on behalf of the European Geosciences Union.

Abstract

Low energy balance closure (EBC) at a particular eddy-covariance flux site increased the uncertainties of carbon, water and energy measurements and thus hampered the urgent research of scaling up and modeling analysis through site combinations. A series of manipulative experiments were conducted in this study to explore the role of net radiation (R_n) in the EBC in relation to spatial variability of vegetation characteristics, source area, sensor type, and dome condition in the Inner Mongolian grassland of Northern China. At all three sites, the daytime peak residual fluxes of EBC were consistently about 100 W m^{-2} regardless of radiometers (i.e., REBS Q7.1 or CNR1). The spatial variability in net radiation was 19 W m^{-2} (5% of R_n) during the day and 7 W m^{-2} (16%) at night, with an average of 13 W m^{-2} (11%) from eight plot measurements across the three sites. Net radiation results were affected more by measurement source area in unclipped heterogeneous system than in clipped homogeneous vegetation. Large area measurement significantly ($P < 0.0001$) increased by 9 W m^{-2} during the day and decreased by 4 W m^{-2} at night in unclipped treatments. With an increase in clipping intensity, net radiation decreased by 25 W m^{-2} (6% of R_n) at midday and 81 MJ m^{-2} (6%) during a growing season with heavier regular clipping than that in unclipped treatments. Additional effort in EBC between 9:00 and 15:00 LT is needed for future research because of high variation. Using this method, the EBC difference derived from the two types of net radiometers was only 6 W m^{-2}. Results from Q7.1 with new domes were higher during the day but lower at night than those with used domes. Overall, the inclusion of the uncertainty in available energy accounted for 60% of the 100 W m^{-2} shortfalls in the lack of closure. Clearly, the unclosed energy balance at these three grassland sites remains significant, with unexplored mechanisms for future research.

BGD

8, 2001–2033, 2011

1 Introduction

The energy balance of the terrestrial surface can be expressed by the first law of thermodynamics, which dictates conservation of energy:

$$R_n = H + LE + G + Q + \varepsilon \quad (1)$$

where R_n is the net radiation, H is the sensible heat flux, LE is the latent heat flux, G is the soil heat flux, Q is the sum of other heat fluxes on the surface (plants, water, etc.) with a small fraction converted to chemical energy through photosynthesis, and ε is any residual flux associated with errors. In grasslands, Q flux is relatively minor due to low and often neglected vegetation mass. With the careful selection of a study site, the residual flux ($\varepsilon = R_n - H - LE - G$) should approximate to zero.

In depth investigations on the energy balance and energy balance closure (EBC) of terrestrial ecosystems have been extensively revisited since the 1990s with rapid increases in the direct measurement of net exchanges of carbon and water using the eddy-covariance (EC) flux tower technology, with which the EBC plays a critical role in assessing the quality of flux measurement (Oncley et al., 2007; Foken, 2008). Within the FLUXNET (http://www.fluxnet.ornl.gov/fluxnet/index.cfm) community, the EBC is considered a key indicator for evaluating the flux data quality of EC measurements (Baldocchi et al., 1996; Goulden et al., 1996; Twine et al., 2000; Wilson et al., 2002; Mauder and Foken, 2006; Finnigan, 2008). The low EBC (i.e., higher portion of missing energy) triggers suspicions that trace gases are not being adequately measured. This would consequently hamper the use of flux data for model validations and/or up scaling exercise (Dugas et al., 1991; Mahrt, 1998; Twine et al., 2000; Turnipseed et al., 2002; Wilson et al., 2002). For example, Wilson et al. (2002) reported that the magnitudes of both CO_2 uptake and respiration were underestimated when the energy imbalance was greater. Similarly, the amount of missing energy correlated negatively with the Bowen ratio (Barr et al., 1994; Brotzge and Crawford, 2003; Chen et al., 2004), suggesting that the turbulent flux measurement had an error when the EBC was low.

BGD
8, 2001–2033, 2011

The energy closure problem is frequently related to low turbulent flux and high available flux ($H + \mathrm{LE} < R_n - G$), potentially due to underestimation of the turbulent flux and/or overestimation of the available energy. Foken (2008), in a review of the EBC problems, reported that the residuals of the EBC in daytime varied from 50–300 W m^{-2}, suggesting that available energy could be 30% higher than turbulent energy (Wilson et al., 2002). In recent years, numerous efforts have been made to explain the specific reasons for the EBCs at diverse flux measurement sites (Brotzge and Crawford, 2003; Oliphant et al., 2004; Sanchez et al., 2010). Yet no commonly accepted theories or underlying mechanisms are accepted by the community. The use of quality net radiometers with sufficient replications and field installations is among many other reasons for conducting our EBC study.

The R_n is the largest flux term in the energy balance (Eq. 1) of a terrestrial ecosystem. Fluctuation of a small percent of R_n would significantly affect the EBC. Previous studies addressing differences among different types of net radiometer sensors (Stannard et al., 1994; Kustas et al., 1998; Brotzge and Duchon, 2000; Twine et al., 2000; Turnipseed et al., 2002; Wilson et al., 2002; Brotzge and Crawford, 2003; Kohsiek et al., 2007) found that some portion of the EBC was due to biased measurements of net radiometers (i.e., different type). Brotage and Crawford (2003) reported that instrumentation error among net radiometers might lead to greater uncertainty in R_n, while Wilson et al. (2002) concluded that, based on inter-comparisons of independently calibrated sensors at several sites, only small differences were due to sensor type.

Inadequate spatial sampling of R_n, especially when patchy vegetation and complex terrains exist, has also been examined as another possible reason for EBC problems (Schmid, 1997; Malhi, 2004). An EC site is conventionally selected to meet the theoretical needs of a large, homogeneous, and flat landscape. While turbulent energy components (i.e., sensible and latent heat fluxes) have a footprint of an entire ecosystem (normally, 50–100 sensor heights from all directions, Chen et al., 2004), net radiation and soil heat fluxes are sampled with a much smaller footprint, with about 100 m^2 for R_n and 10^{-4} m^2 for G. These mismatched measurement footprints would not be a problem

BGD
8, 2001–2033, 2011

when the spatial variation of vegetation, soil, and topography is minimal (i.e., vegetation source area contributes equally; Schmid, 1994, 1997). However, such ideal conditions rarely exist. To improve the EBC, one solution is to increase the sampling numbers of R_n and G (i.e., increasing the measurement footprint) within the larger footprint of the turbulent footprints (Schmid, 1997; Shao et al., 2008).

The contribution of spatially variable G to the EBC was previously addressed (Shao et al., 2008). This paper investigates how spatial variability in R_n affects EBCs through a detailed analysis of vegetation characteristics, instrument maintenance, and source area effects. Three specific questions will be answered through inter/intra-site comparisons and manipulative experiments: (1) What is the magnitude of the spatial variability in R_n at the three EC measurements sites? (2) What are the potential causes of R_n variation within and between our sites? (3) What are the contributions of R_n to EBC at these sites due to its spatial variation caused by heterogeneous vegetation? To answer the above questions, we designed four experiments in a typical grassland type of Inner Mongolia and applied a mobile energy system, which consists of nine net radiometers and other meteorological sensors with three eddy flux towers to record spatially independent R_n and associated surface properties (i.e., vegetation and soil). We specifically hypothesize that the heterogeneity of vegetation structure plays an important role in energy balance closure due to its direct alterations of the outgoing (or reflectance) of short- and long-wave ration that determine the magnitude of net radiation.

2 Sites and methods

2.1 Site descriptions

Experiment 1 was designed to measure R_n at three EC measurement sites, Duolun (site I), Xilinhot (site II) and Dongwu (site III) of Inner Mongolia, Northern China during the growing season of 2006. Experiments 2–4 were conducted at site I during the growing season of 2007 in a manipulative plot that is approximately 1000 m south of the EC tower (Table 1).

The study site involved in Experiments 2–4 was located at Shisanlitan Grassland Ecosystem Restoration Research Station in Duolun County – a semiarid agriculture-pasture transition area in Southeastern Inner Mongolia. The site has a distinct continental climate with a mean annual relative humidity of 61% and a mean annual precipitation 399 mm (375 mm in year 2007), which falls primarily from May to October. The mean annual temperature is 3.3 °C, with a mean monthly temperature ranging from −15.9 °C in January to 19.9 °C in July (1990–2004). Summers are relatively damp and warm while winters are rather cold, dry and windy. The study site was flat with relatively homogenous vegetation within the landscape. The experimental manipulations were conducted in the *Stipa krylovii* grassland that is the most dominant vegetation in the region. The soils are chestnut soils, and below 0.4 m is a mixture of sandy soil and gravel. The site had been fenced since 2001 to prevent large herbivores, such as cattle and sheep, from grazing on the grassland as they had previously. The dominant species include *Stipa krylovii*, *Artemisia frigida*, and *Potentilla acaulis*.

2.2 Experiment 1: spatial variability of R_n within the EC towers

All of the EBC terms in Eq. (1) were directly measured at each of the EC towers (Zhang et al., 2007). R_n was measured by four-component net radiometers CNR1 (Kipp & Zonen, Delft, The Netherlands). The open path EC tower included a fast response three-dimensional ultrasonic anemometer (CSAT3, Campbell Scientific Inc. (CSI), Logan, UT, USA) installed 3 m above the ground and a LI7500 IRGA (InfraRed Gas Analyzer, LiCor Inc., Lincoln, NE, USA) to obtain the LE and H. We arbitrarily laid out a 50 × 50 m^2 plot around the three EC towers to install the mobile energy balance (EB) system, which consists of eight stations in an orthogonal layout with 12.5 m intervals in the four cardinal directions. That is, two stations were installed at distances of 12.5 and 25 m from the center point in each direction. Each station was equipped with a Q7.1 net radiometer (Radiation Energy Balance System (REBS), Seattle, WA, USA) mounted 2.0 m above the ground, two heat flux transducers (HFT3.1, REBS) buried at 0.03 m depth to measure soil heat flux (G_0), and one custom-made T-type copper-constantan thermocouple to measure soil temperature at −0.05 m (T_s). The mobile EB system also included four water content reflectometers (model CS616, CSI) in the four directions at a depth of −0.025 m (upper pole) to record soil volumetric water content (θ), and three E-type chromel-constantan thermocouples for measuring soil surface temperature (T_0). Soil bulk density (ρ_b), from surface to 0.05 m depth, was measured in four replicates in each direction at each site. T_s, T_0, θ and ρ_b were used to calculate the soil layer heat storage (S) above the two HFT3.1s. The sum of G_0 and S is soil heat flux (G). All the Q7.1s were corrected by using the same wind speed derived from an anemometer (05103, CSI) that mounted at 2 m above the ground at each site. Data was collected at 10 s intervals and compiled as 30 min averages with a CR10X datalogger (CSI). The prevailing wind directions were northwest for sites I and II and southwest for site III with an average wind velocity of 3.5, 3.4 and 3.1 m s^{-1} from 1 June to 30 September for sites I, II and III, respectively. Footprint analysis was performed using the methoof Stannard (1997, Eq. (18), P382), resulting an approximately 99% (500 m) or 97% (250 m) of the measured scalar fluxes originated from all the three site towers in each direction (see Shao et al., 2008, for detailed site descriptions and S calculations).

2.3 Experiment 2: vegetation influence

To assess the influences of vegetation on R_n, a manipulative experiment initiated in 2003 near site I but outside the EC tower footprint was used. The experiment was planned in a single-factor design with five clipping treatments and five replications to mimic grazing effects on the grassland: remain shoot 0.02 (R_2), 0.05 (R_5), 0.10 (R_{10}), 0.15 m (R_{15}) and without clipping (R_t, control). Three replicate microclimate stations were installed in each of the R_2, R_{10} and R_t treatments, for a total of nine stations. Continuous measurements of micrometeorological variables began on 3 June (DOY 154) 2007. After four years of continuous clipping, the dominate species changed from tall-stature bunchgrass *Stipa krylovii* (treatment R_t) to short-stature semi-shrub *Artemisia frigida* (treatment R_2). The cover, biomass and biomass-per-cluster in *Stipa* *krylovii*, leaf area index (LAI), green biomass, height, and litter weight in community of R_2 plots were consistently less than those of R_{10} and R_t (Table 2).

The 25 $10 \times 20\,\mathrm{m}^2$ plots were randomly assigned for treatment types and placed with 4 m gaps between the adjacent plots. A push mower (Yard-man 160CC, USA) was used to clip the vegetation in late-August once a year and plants were allowed to grow until the next clipping. The EB system used in Experiment 1 was added with one identical station to measure nine plots simultaneously in the R_2, R_{10} and R_t treatments, respectively, with three replications. The nine stations were distributed randomly but avoided the edge effects (Chen et al., 1992).

2.4 Experiment 3: dome influence

This experiment was designed to detect a potential cause of energy imbalance among sites, the effect of old and new domes. For the first three days (1–3 July), all nine net radiometers (three replicates in treatments R_2, R_{10} and R_t) were with old domes. For the next three days (4–6), we selected one radiometer from R_2, R_{10} and R_t treatments, respectively, and changed them to new domes. For the last three days (7–9), all the other net radiometers were changed to new domes. One measurement in R_2 (net radiometer No. 9) which was last to be changed to a new dome was selected as a benchmark. All the data from the same three days minus the benchmark value were integrated to a diurnal scale to show the measurement differences among net radiometers with old and new domes.

2.5 Experiment 4: influence of the source area

The size of the source area under a radiometer can also be critical, since a large source area will often include more diverse land surfaces, especially when disturbances (clipping) are involved. Three paired Q7.1 net radiometers were randomly selected for 12–20 July, with one Q7.1 raised to 1 m higher than the other during a four-day study period (Table 1).

BGD
8, 2001–2033, 2011

The source area of a radiometer with hemispherical windshield can be calculated as (Stannard et al., 1994),

$$A = 1 - [(R/h)^2 + 1]^{-1} \quad (2)$$

where A is the relative contribution to the measured flux signal from a partial source area (centered below the net radiometer) of radius R for net radiometer height above the canopy of h. When $R/h = \infty$, $A = 1$. In experiments 2 and 3, as $R/h > 10$, ≈ 99% contributed from each of the measured clipping plots; while in experiment 4, $R/h = 3.3$, therefore $A = 92\%$. The plot area in our study was large enough for all three experiments. Descriptions of net radiometer deployments of experiments 1–4 are listed in Table 1.

2.6 Inter-comparison

In addition to the factory calibration of Q7.1 at the beginning of experiment 1, one week field inter-comparison (Halldin and Lindroth, 1992) was also conducted during experiment 2 (Table 3). Experiment 1 was conducted in the summer of 2006 with the new eight factory calibrated Q7.1s. We did not make an additional effort in calibrating them. These Q7.1s were moved to three sites (I, II and III), and then settled in site I until experiments 2, 3 and 4 were conducted. At this time, nine Q7.1s were randomly divided into three groups and operated side by side.

2.7 Eddy-covariance data processing and gap filling

The EC data were processed with the "EC Processor" software (Noormets et al., 2007), which were corrected by the double rotation method using the Webb-Pearman-Leuning expression (Paw et al., 2000; Mauder and Foken, 2006). We also removed anomalous or spurious data that were caused by sensor malfunction, sensor maintenance, rainfall events, IRGA calibration, power failure, etc. Data from stable nocturnal periods were also excluded, specifically when the friction velocity u^* (Goulden et al., 1996; Moncrieff et al., 1996) was $< 0.15\,\mathrm{m\,s^{-1}}$ (Zhang et al., 2007). Consequently, 29, 21 and

Discussion Paper | Discussion Paper | Discussion Paper | Discussion Paper |
BGD
8, 2001–2033, 2011
Net radiation with energy balance closure
C. Shao et al.
Title Page
Abstract Introduction
Conclusions References
Tables Figures
◀◀ ▶▶
◀ ▶
Back Close
Full Screen / Esc
Printer-friendly Version
Interactive Discussion

28% of the July–September data obtained from our EC systems from sites I, II and III, respectively, were discarded in experiment 1. These introduced data gaps that were filled following the methods of Falge et al. (2001), using sensible and latent heat fluxes. Linear interpolation was used to fill the gaps that were less than 2 h by calculating an average of the values immediately before and after the data gaps. Larger data gaps were filled using empirical relationships (look-up tables). For each site, one look-up table, which sorted by photosynthetic photon flux density (PPFD) and vapor pressure deficit (VPD), was created from 1 July to 30 September and, after gap filling the data for corresponding days, were extracted and analyzed with the net radiation and soil heat flux data.

2.8 Data analysis

We analyzed the energy balance residual and applied linear regression to explore the spatial variability in R_n contributing to EBC in Experiment 1. First, the data from 12, 16 and 17 days at sites I, II and III, respectively, were compiled into 30 min averages to illustrate the residual fluxes of EBC (i.e., ε). Then the data was examined using an ordinary least square (OLS) linear regression by relating dependent turbulence energy ($H+\mathrm{LE}$) and independent available energy (R_n-G). The mean values of the 30 min R_n and G from eight replicated measurements were calculated at each site. The mean values of R_n were used to compare the closures resulting from Q7.1 with those from CNR1 at the EC towers. The maximum and minimum values were used to illustrate the spatial variability of R_n and its contribution to the EBC. The mean values of G from sixteen replications were used to calculate the EBC. Rainy days were deliberately avoided, because the turbulent energy instruments would not work well at those times. For experiments 2–4, all the 30 min experimental period data were also integrated and examined on a diurnal scale. The paired-T test (SPSS 11.0 software) was used to analyze R_n deployment by height to find its contribution to the EBC. R_n differences among treatments/plots were used to examine the influences of vegetation, dome, and source area.

3 Results

3.1 Spatial variability of R_n

The ε averaged 19 W m^{-2} (i.e., 5% of R_n) during the day and 7 W m^{-2} (16%) at night across the three sites due to the spatial variability in R_n (Table 4, Fig. 1). The day time ε were 48, 68 and 67 W m^{-2} due to the maximum R_n for sites I, II and III, respectively, and 33, 48 and 47 W m^{-2} due to the minimum R_n (Table 4, Fig. 1). Altogether, the spatial variability in R_n contributing to the EBC was approximately 13 W m^{-2} or 11% of the daily mean R_n (Table 4). A 4% OLS slope difference (0.81 and 0.85) was found from the replicated R_n sampling (i.e., spatial variability). The OLS slopes for sites I, II and III, were 0.90, 0.86 and 0.79 for the minimum R_n, respectively, and 0.89, 0.79 and 0.75 for the maximum R_n. The wet site (i.e., site I) had the highest OLS slopes for both day and night.

3.2 Sensor influence

The R_n values from the Q7.1 and CNR1 net radiometers were different and varied by time. The residual fluxes of the EBC (i.e., ε) were similar between the two radiometers during the day but higher (less negative) from the Q7.1 at night at all three sites (Fig. 2). In the daytime, especially from 9:00 to 15:00 LT, only 6 W m^{-2} difference among the three sites was found. However, larger differences appeared at night which reached up to 21 W m^{-2} at sites I and III, whereas at site II, the difference was 11 W m^{-2}.

The OLS linear regression showed similar results, with 5% OLS slope difference for the Q7.1 measurements (0.84) and the CNR1 (0.79) across the three sites (Fig. 3). The Q7.1 provided an OLS slope of 0.77–0.90, while the CNR1 had slopes of 0.70–0.84. When only the data from 9:00 to 15:00 LT was used for sites I, II and III, the OLS slopes were 0.89, 0.85 and 0.75 for the Q7.1 measurements, respectively, and 0.88, 0.87 and 0.70 for the CNR1 measurements. The average difference of all three sites was 3%.

BGD
8, 2001–2033, 2011

3.3 Vegetation influence

With increase in clipping intensity, R_n decreased during most of the daytime throughout the growing season (Fig. 4). At midday, the average R_n values were 413, 395 and 388 W m^{-2} for the R_t, R_{10} and R_2 treatments over the growing season, respectively. The R_n in R_2 was nearly 6% lower than in R_t treatments both at midday and by daily total. Over the growing season, the total R_n were 1409, 1331 and 1328 MJ m^{-2} for R_t, R_{10} and R_2, respectively, i.e., in the heavily mowed treatment (R_2) decreased by 6% (or about 81 MJ m^{-2}) as compared to the reference.

3.4 Dome influence

The R_n values were obviously influenced by dome condition (Fig. 5). R_n with new domes were higher during the day and lower at night than those with used domes (i.e., deployed in the field for ten months). The peak R_n values with new domes were about 60, 40 and 20 W m^{-2} higher than those with used domes in R_t, R_{10} and R_2 treatments, respectively. After dome replacement, R_n in R_t treatment showed the highest increase while R_n in R_2 treatment increased the least. On average, used domes underestimated the R_n by as much as 25 W m^{-2} in daytime and overestimated by 10 W m^{-2} at night (Fig. 5). When simultaneous measurements from used and new domes were compared, we found that the difference was $<$ 2–3 W m^{-2} at night in the R_2 and R_t treatments, but 10 W m^{-2} in the R_{10} treatment.

3.5 Source area influence

The size of source, changed by deploying Q7.1 at different heights, did not show a significant influence in R_2 and R_{10}, except in R_t treatments (Fig. 6). With R_t treatment, R_n was 9 W m^{-2} during the day (9:00–15:00 LT, $P < 0.0001$) and 4 W m^{-2} at night (21:00–3:00 LT) between the two heights. In R_2 and R_{10} treatments, however, the R_n differences were generally $<$ 2 W m^{-2} throughout the day.

BGD
8, 2001–2033, 2011

4 Discussion

4.1 Inter-comparison

Our primary focus of this study is not to prove the superiority of one net radiometer over another, but seek potential sources of missing R_n energy within the EBC at multiple sites where vegetation structure had been manipulated. Each kind of commercial instruments had its own characters. Different types, models, and corrections of/for net radiometers could be a reason for the unclosed energy balance which was evident through several comparison studies (Stannard et al., 1994; Kustas et al., 1998; Brotzge and Duchon, 2000; Twine et al., 2000; Turnipseed et al., 2002; Wilson et al., 2002; Brotzge and Crawford, 2003; Kohsiek et al., 2007; Foken, 2008). In the last 15 years, much has been done to increase the accuracy of the radiation measurements (Wilson et al., 2002; Kohsiek et al., 2007; Foken, 2008). The regression slope of the comparisons remained constant over the sampling period for the three treatments, suggesting that the Q7.1 is a stable sensor (Table 3). Further evidences showing small difference (Fig. 5) at the R_2 among Q7.1 radiometers (0.5 W m^{-2} during 9:00–15:00 LT and 1 W m^{-2} between 21:00–3:00 LT) are likely due to the more homogeneous vegetation. Clearly, the error related with the different Q7.1 could be neglected with good maintenance. However, in the early evening, the Q7.1 can produce occasion spikes (Figs. 5 and 6).

4.2 Spatial variability of R_n and the EBC

The spatial variability of the R_n measured from multiple Q7.1 sensors was 19 W m^{-2} (5% of R_n) during the day and 7 W m^{-2} (16%) at night, with a daily average of 13 W m^{-2} (11%) or a 4% OLS slope. This variability might be due to the differences in vegetation structure, soil characteristics, microclimates and/or instrumental error among the eight plots at each site. However, the spatial variability in available energy is still smaller to account for the lack of closure. The turbulent flux is systematically lower by 100 W m^{-2}

BGD
8, 2001–2033, 2011

at peak time than the available energy (Figs. 1 and 2). The uncertainty in R_n could contribute to a systematic error of about 20 W m^{-2}, or 5% of R_n which is in consistent with the report by Twine et al. (2000) of 6% of midday and mid-season R_n at a grass site in Oklahoma. The uncertainty in soil heat flux could contribute another 40 W m^{-2} of error to the available energy (Shao et al., 2008). Altogether, the inclusion of the uncertainty in available energy accounted for about 60% of the 100 W m^{-2} shortfall in the lack of closure. Clearly, the unclosed energy balance at these three grassland sites remains real and there remain unexplored mechanisms. Yet, it is unlikely that improper measurement of R_n during the daytime is responsible for the energy imbalance because both CNR1 and Q7.1 were in relative accordance during the course of the study (Turnipseed et al., 2002).

We designed a large scale plot (50 × 50 m^2) with eight Q7.1s and sixteen soil heat flux plates to quantify the spatial variability in R_n and G approximately to match with the source area with H and LE. The mean R_n and G stood in reasonably well for the large scale realities. There still existed 47 ± 16, 50 ± 13 and 70 ± 15 W m^{-2} of the energy balance at midday that could not be explained at sites I, II and III, respectively. Even with all of the spatial uncertainties included, an imbalance of ∼20 W m^{-2} still existed, perhaps due to other instrumental, operational, and flow based errors (Finnigan, 2008). Examples of these errors are H, LE, or both of the turbulent fluxes at either low- and/or high-frequency and mean vertical or horizontal advection of scalar quantities. Gash et al. (2003) and van der Molen et al. (2004) argued that turbulence energy from a sonic anemometer (co)sine errors was a potential source, while Aubinet et al. (2000) and Foken et al. (2001) pointed out that the time lag among different energy fluxes measurement need to be considered. Twine et al. (2000) also calculated that the uncertainties from R_n and G could only account for half of their imbalance 130 W m^{-2} in grassland at midday.

BGD
8, 2001–2033, 2011

4.3 Sensor differences

The thick plastic domes on Q7.1 might have a sufficiently low thermal transmissivity resulting in underestimated incident thermal sky radiation (Twine et al., 2000). Additionally, the CNR1 measured a wider spectrum of wavelengths than Q7.1 (Brotzge and Duchon, 2000), which could also introduce additional bias, particularly in the nighttime. There is no doubt that this discrepancy would lead to a large variation in ε at night. In this study, the R_n of the CNR1 were significantly lower (10–20 $W m^{-2}$) at night than those of the Q7.1, with the OLS slope varying approximately 5% (Fig. 2). Brotzge and Duchon (2000) and Kohsiek et al. (2007) compared these two types of radiometer and found a similar difference at night (15 $W m^{-2}$). In our study, the regression slope remained constant during the study period at all three sites (1.04 ± 0.02), using the value of Q7.1 as the independent variable. This suggests that the calibrations of the two instrument types remained constant (Turnipseed et al., 2002), with regression slopes of 1.00 ± 0.01 in the daytime (9:00–15:00 LT) and 1.31 ± 0.07 at night (21:00–3:00 LT). Nighttime measurements of R_n, however, showed substantial discrepancies between the two sensors-close to 1.25 reported by Turnipseed et al. (2002) in a forest where the authors suspected as an error in the "long-wavelength measurement of one or both radiometers". Other authors (Halldin and Lindroth, 1992; Hodges and Smith, 1997; Brotzge and Duchon, 2000; Brotzge and Crawford, 2003; Oncley et al., 2007) also noticed the discrepancies between different instruments. The magnitudes of nocturnal turbulent heat fluxes are typically underestimated with the EC method, as turbulence generally low. The underestimation (less negative) of nocturnal R_n value from Q7.1 would further increase EBC. Thus this difference must be taken into account when comparing and calculating EBC among or within sites.

The different EBC could also occur at different time scales. On a half-hourly scale, for example at site I, it showed the same daytime EBC, while the ε value determined by the Q7.1 was closer to zero at night. Therefore, we conclude that multiple Q7.1 measurements provided much "better closure" (Fig. 2a) because of the underestimation

BGD
8, 2001–2033, 2011

of the magnitude of Rn with the Q7.1 during nighttime. However, on a daily scale, it seemed that CNR1 provided better measurements. On a typical day (11 July), the daily imbalance yielded 1.44 MJ m^{-2} d^{-1} using Q7.1 while only 0.63 MJ m^{-2} d^{-1} using CNR1.

Due to the difference between the Q7.1 and CNR1, a method in comparing the EBCs within and among sites at a specific period from 9:00 to 15:00 LT during the daytime would be useful to provide definite results both in residual and OLS regression methods. This is because during this period, the sensors (net radiometer, sensible and latent heat measurements) usually worked in their best conditions (e.g., high friction velocity). Different kinds of gap-filling strategies (Falge et al., 2001) in H and LE usually impede further EBC analysis. Furthermore, in the early morning and evening when net radiation is changing most rapidly, the magnitude of storage heat in the soil, air and biomass can approach that of R_n (Moore and Fisch, 1986). However, toward the midday, the storage heat is less important (McCaughey, 1982). Using this method, the effect of differences between instruments would be partially avoided.

4.4 Dome condition effects on EBC

While comparing the results among new and used domes, the difference between new domes was negligible. With new domes, the higher R_n (25 W m^{-2}) was recorded during the day but lower values (10 W m^{-2}) at night, resulting an increased energy imbalance at hourly scale. Because all the R_n differences were calculated by subtracting R_n values from the heavily clipped R_2 (net radiometer No. 9), the maximum difference between old and new domes was ~30 W m^{-2} (i.e., approximately 5% of net radiation; Fig. 5 R_2). Based on the comparisons between the Q7.1 net radiometers on 18–25 July 2007, which just after experiment 3, the results showed that Q7.1 with new domes changed upper and bottom ones together are much more reliable and highly recommended (Fig. 5 for NN). We concur with the recommendation of the manufacture that dome replacement of three to six months for the convictive EBC. We found that the ε can be large to 30 W m^{-2} associated with the dome replacement.

4.5 Potential causes of R_n measurements for nonclosure

In addition to the spatial variability resulted from vegetation, radiometer type and dome condition, source area could also be responsible for inaccurate R_n measurements. In the unclipped plot, R_n might be higher due to a lower albedo in comparison to the clipped one (Li et al., 2006). The Student-t test, with a 0.05 level of significance, was used in previous studies to examine the differences between samples from the different clipping treatments. The maximum contrast in vegetation was found between sample treatments R_t and R_2 with the latter having less LAI and green biomass (Table 2). This explained 6% difference in R_n that was recorded in experiment 2 (Fig. 4), and also the peak difference of ~10–20 W m^{-2} between R_t and R_2 in experiments 3 and 4 (Figs. 5 and 6) in our steppe grassland sites.

The source area experiment indicated that Q7.1 deployment needs to be high enough to record reliable R_n, especially under heterogeneous surface. The typical deployment height of 1.5–2.0 m seemed to not be adequate to integrate across vegetation heterogeneity (Stannard et al., 1994). An error would appear with low installation height of radiometers because the sensor could not receive the representative long- and short-wave reflections from the surface. However, Lloyd et al. (1997) pointed out that as the height of the net radiometer increases, the measurement would be degraded by long wave losses in the air layer between the surface and the measurement height. Improved comparisons between radiometers deployed at 0.5 m and 1.5 m were found in homogenous R_2, but not in heterogeneous R_t in experiment 4. This suggests that the sensor height needs to be site specific.

From Table 4, Figs. 2 and 3, compare site II, III with I, when LE was larger the energy closure was better. The mismatch of energy fluxes (Shao et al., 2008) and underestimate LE (Dugas et al., 1991) in arid sites should responsible for this imbalance. Because sensible heat fluxes between both systems compared better than latent heat fluxes (Schlesinger et al., 1996), we do agree with the view of the instrument could cause bigger error when LE was lower (Stannard et al., 1994). This point need to be

BGD
8, 2001–2033, 2011

studied further. The closure issue becomes even more important upon consideration of the long-term water balance. Twine et al. (2000) summed over a period of 15 days from 4 EC systems and drew a conclusion that the evapotranspiration would be significantly overestimated by calculating LE as the residual of the energy budget. This is also supported by others (Dugas et al., 1991; Nie et al., 1992; Kampf et al., 2005). So to our study, it is a risk to use eddy-covariance residual_method to estimate the LE because there were more uncertainties from R_n, G, S and other heat sinks. This coincided with others (Twine et al., 2000; Wilson et al., 2002) that each fluxes should be analyzed separately. And we also found the EBC was better in night rather than in the midday, especially in the photosynthesis time, this seemed if more photosynthesis heat storage was neglected which cause the non-closure. But if so, the EBC should better in less vegetation plot (e.g. site III) or in leafless seasons, in fact, it is not the truth. This study only addressed spatial variations of R_n and soil heat flux contribute to the energy balance closure during the grasslands growth reason, much more data sets under different conditions (e.g. in winter, before leaf emergence and after defoliation) must be analyzed in a similar way to create new findings. At the same time, from this study, we found that the energy balance closure was better under conditions of higher soil moisture, higher LE, higher vegetation cover, lower H and lower latitude. But what is the truth, also need to be studied further.

5 Conclusions and perspectives

Net radiation contributions to the energy balance closure were examined through four experiments in grassland where eddy-covariance towers had been installed since 2005. Vegetation heterogeneity, sensor type, and dome condition all played critical roles in the EBC of our study sites. Despite the fact that soil heat which is estimated too low and net radiation estimated too high could not be excluded, the spatial variability quantity in net radiation is less than that in soil heat flux, and the sum of these two energy fluxes (i.e., available energy) accounted for 60% of the missing energy. The

BGD
8, 2001–2033, 2011

other portion of missing energy remains at large, near 40 W m^{-2} at the daytime peak time. More effort under different conditions (e.g., winter, spring, and fall when different phenological vegetation exist, different weather conditions, and long time scales) must be made in a similar way to reach a comprehensive understanding of EBC. For example, we noticed that the EBC was better under higher soil moisture conditions, high LE, high vegetation cover, low H, and low latitude. New experiments including additional quality assurance like traceable reference R_n are needed to systematically explore the mechanisms or empirical relationships.

In view of the net radiation measurement, the differences among different types of instruments are also important in EBC. Results would become confusing and unreliable if these differences were neglected. Due to the difference between the Q7.1 and CNR1 at night, an additional effort in comparing EBCs within and among sites during 9:00 to 15:00 LT would be useful to provide us with more insights on EBC due to the lower uncertainties during this period. However, other types of net radiometers or instruments, whether or not they are suitable to this specific period method, should also be studied when considering the EBC question and integrating flux data.

Acknowledgements. This study was supported by the Natural Science Foundation of China (30928002), NASA-NEWS Program (NN-H-04-Z-YS-005-N), the Outstanding Overseas Scientists Team Project of CAS, and the State Key Basic Research Development Program of China (2007CB106800). We would like to thank Shiping Chen and Jianfeng Liu for providing eddy-covariance data, Asko Noormets for "EC processor" software, and Yibo Shi for constructive advice on maintaining the mobile energy system. We would also like to thank Xin Li and Zhichun Yan for their assistance in fieldwork. We greatly appreciate the careful review by Valerie Pinkerton, Lisa Delp and Alona Gutman.

BGD
8, 2001–2033, 2011

References

Aubinet, M., Grelle, A., Ibrom, A., Rannik, U., Moncrieff, J., Foken, T., Kowalski, A. S., Martin, P. H., Berbigier, P., Bernhofer, C., Clement, R., Elbers, J., Granier, A., Grunwald, T., Morgenstern, K., Pilegaard, K., Rebmann, C., Snijders, W., Valentini, R., and Vesala, T.: Estimates of the annual net carbon and water exchange of forests: the EUROFLUX methodology, Adv. Ecol. Res., 30, 113–175, 2000.

Baldocchi, D. D., Valentini, R., Running, S., Oechel, W., and Dahlman, R.: Strategies for measuring and modelling carbon dioxide and water vapour fluxes over terrestrial ecosystems, Global Change Biol., 2, 159–168, 1996.

Barr, A. G., King, K. M., Gillespie, T. J., Denhartog, G., and Neumann, H. H.: A comparison of bowen-ratio and eddy-correlation sensible and latent-heat flux measurements above deciduous forest, Bound.-Lay. Meteorol., 71, 21–41, 1994.

Brotzge, J. A. and Crawford, K. C.: Examination of the surface energy budget: a comparison of eddy correlation and Bowen ratio measurement systems, J. Hydrol., 4, 160–178, 2003.

Brotzge, J. A. and Duchon, C. E.: A field comparison among a domeless net radiometer, two four-component net radiometers, and a domed net radiometer, J. Atmos. Ocean. Tech., 17, 1569–1582, 2000.

Chen, J. Q., Franklin, J. F., and Spies, T. A.: Vegetation responses to edge environments in old-growth douglas-fir forests, Ecol. Appl., 2, 387–396, 1992.

Chen, J. Q., Paw, U., Ustin, S. L., Suchanek, T. H., Bond, B. J., Brosofske, K. D., and Falk, M.: Net ecosystem exchanges of carbon, water, and energy in young and old-growth Douglas-fir forests, Ecosystems, 7, 534–544, 2004.

Dugas, W. A., Fritschen, L. J., Gay, L. W., Held, A. A., Matthias, A. D., Reicosky, D. C., Steduto, P., and Steiner, J. L.: Bowen-ratio, eddy-correlation, and portable chamber measurements of sensible and latent-heat flux over irrigated spring wheat, Agr. Forest Meteorol., 56, 1–20, 1991.

Falge, E., Baldocchi, D., Olson, R., Anthoni, P., Aubinet, M., Bernhofer, C., Burba, G., Ceulemans, G., Clement, R., Dolman, H., Granier, A., Gross, P., Grunwald, T., Hollinger, D., Jensen, N. O., Katul, G., Keronen, P., Kowalski, A., Lai, C. T., Law, B. E., Meyers, T., Moncrieff, J., Moors, E., Munger, J. W., Pilegaard, K., Rannik, U., Rebmann, C., Suyker, A., Tenhunen, J., Tu, K., Verma, S., Vesala, T., Wilson, K., and Wofsy, S.: Gap filling strategies for long term energy flux data sets, Agr. Forest Meteorol., 107, 71–77, 2001.

BGD
8, 2001–2033, 2011

Finnigan, J.: An introcuction to flux measurements in difficult conditions, Ecol. Appl., 18, 1340–1350, 2008.
Foken, T.: The energy balance closure problem: an overview, Ecol. Appl., 18, 1351–1367, 2008.
Foken, T., Wichura, B., Klemm, O., Gerchau, J., Winterhalter, M., and Weidinger, T.: Micrometeorological measurements during the total solar eclipse of 11 August 1999, Meteorol. Z., 10, 171–178, 2001.
Gash, J. H. C. and Dolman, A. J.: Sonic anemometer (co)sine response and flux measurement I. The potential for (co)sine error to affect sonic anemometer-based flux measurements, Agr. Forest Meteorol., 119, 195–207, 2003.
Goulden, M. L., Munger, J. W., Fan, S. M., Daube, B. C., and Wofsy, S. C.: Measurements of carbon sequestration by long-term eddy covariance: methods and a critical evaluation of accuracy, Global Change Biol., 2, 169–182, 1996.
Halldin, S. and Lindroth, A.: Errors in net radiometry – comparison and evaluation of 6 radiometer designs, J. Atmos. Ocean. Tech., 9, 762–783, 1992.
Hodges, G. B. and Smith, E. A.: Intercalibration, objective analysis, intercomparison and synthesis of BOREAS surface net radiation measurements, J. Geophys. Res.-Atmos., 102, 28885–28900, 1997.
Kampf, S. K., Tyler, S. W., Ortiz, C. A., Munoz, J. F., and Adkins, P. L.: Evaporation and land surface energy budget at the Salar de Atacama, Northern Chile, J. Hydrol., 310, 236–252, 2005.
Kohsiek, W., Liebethal, C., Foken, T., Vogt, R., Oncley, S. P., Bernhofer, C., and Debruin, H. A. R.: The energy balance experiment EBEX-2000. Part III: Behaviour and quality of the radiation measurements, Bound.-Lay. Meteorol., 123, 55–75, 2007.
Kustas, W. P., Prueger, J. H., Hipps, L. E., Hatfield, J. L., and Meek, D.: Inconsistencies in net radiation estimates from use of several models of instruments in a desert environment, Agr. Forest Meteorol., 90, 257–263, 1998.
Li, S. G., Eugster, W., Asanuma, J., Kotani, A., Davaa, G., Oyunbaatar, D., and Sugita, M.: Energy partitioning and its biophysical controls above a grazing steppe in Central Mongolia, Agr. Forest Meteorol., 137, 89–106, 2006.
Lloyd, C. R., Bessemoulin, P., Cropley, F. D., Culf, A. D., Dolman, A. J., Elbers, J., Heusinkveld, B., Moncrieff, J. B., Monteny, B., and Verhoef, A.: A comparison of surface fluxes at the HAPEX-Sahel fallow bush sites, J. Hydrol., 189, 400–425, 1997.

Mahrt, L.: Flux sampling errors for aircraft and towers, J. Atmos. Ocean. Tech., 15, 416–429, 1998.
Malhi, Y., McNaughton, K., and Von Randow, C.: Low frequency atmospheric transport and surface flux measurements, Handbook of Micrometeorology, edited by: Lee, X., Massman, W., and Law, B., Kluwer Academic Publishers, Netherlands, 101–118, 2004.
Mauder, M. and Foken, T.: Impact of post-field data processing on eddy covariance flux estimates and energy balance closure, Meteorol. Z., 15, 597–609, 2006.
McCaughey, J. H.: Spatial variability of net radiation and soil heat flux density on two logged sites at Montmorency, Quebec, J. Appl. Meteorol., 21, 777–787, 1982.
van der Molen, M. K., Gash, J. H. C., and Elbers, J. A.: Sonic anemometer (co)sine response and flux measurement – II. The effect of introducing an angle of attack dependent calibration, Agr. Forest Meteorol., 122, 95–109, 2004.
Moncrieff, J. B., Malhi, Y., and Leuning, R.: The propagation of errors in long-term measurements of land-atmosphere fluxes of carbon and water, Global Change Biol., 2, 231–240, 1996.
Moore, C. J. and Fisch, G.: Estimating heat-storage in Amazonian tropical forest, Agr. Forest Meteorol., 38, 147–168, 1986.
Nie, D., Kanemasu, E. T., Fritschen, L. J., Weaver, H. L., Smith, E. A., Verma, S. B., Field, R. T., Kustas, W. P., and Stewart, J. B.: An intercomparison of surface-energy flux measurement systems used during FIFE 1987, J. Geophys. Res.-Atmos., 97, 715–724, 1992.
Noormets, A., Chen, J., and Crow, T. R.: Age-dependent changes in ecosystem carbon fluxes in managed forests in Northern Wisconsin, USA, Ecosystems, 10, 187–203, 2007.
Oliphant, A. J., Grimmond, C. S. B., Zutter, H. N., Schmid, H. P., Su, H. B., Scott, S. L., Offerle, B., Randolph, J. C., and Ehman, J.: Heat storage and energy balance fluxes for a temperate deciduous forest, Agr. Forest Meteorol., 126, 185–201, 2004.
Oncley, S. P., Foken, T., Vogt, R., Kohsiek, W., DeBruin, H. A. R., Bernhofer, C., Christen, A., van Gorsel, E., Grantz, D., Feigenwinter, C., Lehner, I., Liebethal, C., Liu, H., Mauder, M., Pitacco, A., Ribeiro, L., and Weidinger, T.: The energy balance experiment EBEX-2000. Part I: Overview and energy balance, Bound.-Lay. Meteorol., 123, 1–28, 2007.
Paw, U. K. T., Baldocchi, D. D., Meyers, T. P., and Wilson, K. B.: Correction of eddy-covariance measurements incorporating both advective effects and density fluxes, Bound.-Lay. Meteorol., 97, 487–511, 2000.

BGD
8, 2001–2033, 2011
Net radiation with energy balance closure
C. Shao et al.

Sánchez, J. M., Caselles, V., and Rubio, E. M.: Analysis of the energy balance closure over a FLUXNET boreal forest in Finland, Hydrol. Earth Syst. Sci., 14, 1487–1497, doi:10.5194/hess-14-1487-2010, 2010.

Schlesinger, W. H., Raikes, J. A., Hartley, A. E., and Cross, A. F.: On the spatial pattern of soil nutrients in desert ecosystems, Ecology, 77, 1270–1270, 1996.

Schmid, H. P.: Source areas for scalars and scalar fluxes, Bound.-Lay. Meteorol., 67, 293–318, 1994.

Schmid, H. P.: Experimental design for flux measurements: matching scales of observations and fluxes, Agr. Forest Meteorol., 87, 179–200, 1997.

Shao, C. L., Chen, J. Q., Li, L. H., Xu, W. T., Chen, S. P., Gwen, T., Xu, J. Y., and Zhang, W. L.: Spatial variability in soil heat flux at three Inner Mongolia steppe ecosystems, Agr. Forest Meteorol., 148, 1433–1443, 2008.

Stannard, D. I.: A theoretically based determination of Bowen-ratio fetch requirements, Bound.-Lay. Meteorol., 83, 375–406, 1997.

Stannard, D. I., Blanford, J. H., Kustas, W. P., Nichols, W. D., Amer, S. A., Schmugge, T. J., and Weltz, M. A.: Interpretation of surface flux measurements in heterogeneous terrain during the Monsoon'90 experiment, Water Resour. Res., 30, 1227–1239, 1994.

Turnipseed, A. A., Blanken, P. D., Anderson, D. E., and Monson, R. K.: Energy budget above a high-elevation subalpine forest in complex topography, Agr. Forest Meteorol., 110, 177–201, 2002.

Twine, T. E., Kustas, W. P., Norman, J. M., Cook, D. R., Houser, P. R., Meyers, T. P., Prueger, J. H., Starks, P. J., and Wesely, M. L.: Correcting eddy-covariance flux underestimates over a grassland, Agr. Forest Meteorol., 103, 279–300, 2000.

Wilson, K. B., Goldstein, A., Falge, E., Aubinet, M., Baldocchi, D., Berbigier, P., Bernhofer, C., Ceulemans, R., Dolman, H., Field, C., Grelle, A., Ibrom, A., Law, B. E., Kowalski, A., Meyers, T., Moncrieff, J., Monson, R., Oechel, W., Tenhunen, J., Valentini, R., and Verma, S.: Energy balance closure at FLUXNET sites, Agr. Forest Meteorol., 113, 223–243, 2002.

Zhang, W. L., Chen, S. P., Chen, J., Wei, L., Han, X. G., and Lin, G. H.: Biophysical regulations of carbon fluxes of a steppe and a cultivated cropland in semiarid Inner Mongolia, Agr. Forest Meteorol., 146, 216–229, 2007.

BGD

8, 2001–2033, 2011

Table 1. Net radiometers and their deployments in the four experiments in this study.

Experiment		Period of measurement	Sensor used	Height
1	Site I	9–29 Jul 2006	Eight Q7.1s; one CNR1	Q7.1 2m; CNR1 4 m
	Site II	31 Jul–20 Aug 2006	Eight Q7.1s; one CNR1	Q7.1 2 m; CNR1 4 m
	Site III	21 Aug–15 Sep 2006	Eight Q7.1s; one CNR1	Q7.1 2 m; CNR1 3.5 m
2		3–30 Jun; 26 Jul–31 Oct 2007	Nine Q7.1s	0.3–0.5 m above the canopy
3		1–9 Jul 2007	Nine Q7.1s	0.5 m above the canopy
4		10–17 Jul 2007	Six Q7.1s	Small 0.5 m; large 1.5 m

BGD
8, 2001–2033, 2011

Table 2. Vegetation characteristics at growing seasonal peak time for clipping treatments where experiments 2, 3 and 4 were conducted. R_2, R_{10} and R_t showed biomass removal by clipping shoots at heights of 0.02 m, 0.10 m, respectively, once a year in late August since 2003 and no clipping. Values (mean ±1 SE) designated by the same letter (a, b or c) are not significantly different at $P = 0.05$ among treatments.

Treat-ment	Vegetation cover (%)	LAI	Living Biomass ($g\,m^{-2}$)	Litter ($g\,m^{-2}$)	Stand dead ($g\,m^{-2}$)	Average height of vegetation (m)	Number of species
R_2	54 ± 2a	0.34 ± 0.02a	66 ± 8a	48 ± 8a	25 ± 4a	0.04 ± 0.01a	15 ± 1a
R_{10}	49 ± 2a	0.38 ± 0.02a	76 ± 10a	58 ± 17a	24 ± 1a	0.09 ± 0.01b	14 ± 2a
R_t	48 ± 5a	0.48 ± 0.02b	112 ± 7b	130 ± 14b	177 ± 19b	0.23 ± 0.02c	12 ± 1b

BGD
8, 2001–2033, 2011
Net radiation with energy balance closure
C. Shao et al.

Table 3. Inter-comparison between the Q7.1 net radiometers on 18–25 July 2007.

Between*	OLS slope	Intercept	r^2
1, 2	0.98	−0.64	0.999
1, 3	0.99	−1.64	1.000
2, 3	1.01	−0.37	0.999
4, 5	0.99	1.53	1.000
4, 9	0.99	1.19	1.000
5, 9	1.01	−0.12	1.000
6, 7	0.98	0.76	1.000
6, 8	0.99	0.99	1.000
7, 8	1.01	0.12	1.000
Mean (SE)	0.99 (0.00)	0.20 (0.34)	1.00 (0.00)

* In the first column, the first value is the independent variable and the second value is dependent variable when making the linear regression. r^2 is the coefficient of determination.

Discussion Paper | Discussion Paper | Discussion Paper | Discussion Paper |

BGD

8, 2001–2033, 2011

Net radiation with energy balance closure

C. Shao et al.

Table 4. Energy balance closure residuals (ε, W m^{-2}) resulted from the spatial variability in R_n at the three grassland sites (I, II and III). Average row shows the mean ε spatial variability of the three sites. The number in brackets is the percentage of ε/R_n;

Site	Midday	Midnight	Day*	Night*	Day and night
I	38 ~ 54 (3)	−10 ~ −1 (20)	33 ~ 48 (3)	−7 ~ 2 (20)	13 ~ 25 (12)
II	65 ~ 87 (5)	1 ~ 7 (13)	48 ~ 68 (5)	1 ~ 7 (14)	25 ~ 38 (9)
III	57 ~ 80 (6)	−11 ~ −4 (16)	47 ~ 67 (6)	−6 ~ 1 (15)	20 ~ 34 (11)
Average	20 (5)	7 (16)	19 (5)	7 (16)	13 (11)

* Day and night refer to 9:00–15:00 and 21:00–3:00 LT, respectively. Data are derived from Experiment 1.

BGD
8, 2001–2033, 2011
Net radiation with energy balance closure
C. Shao et al.

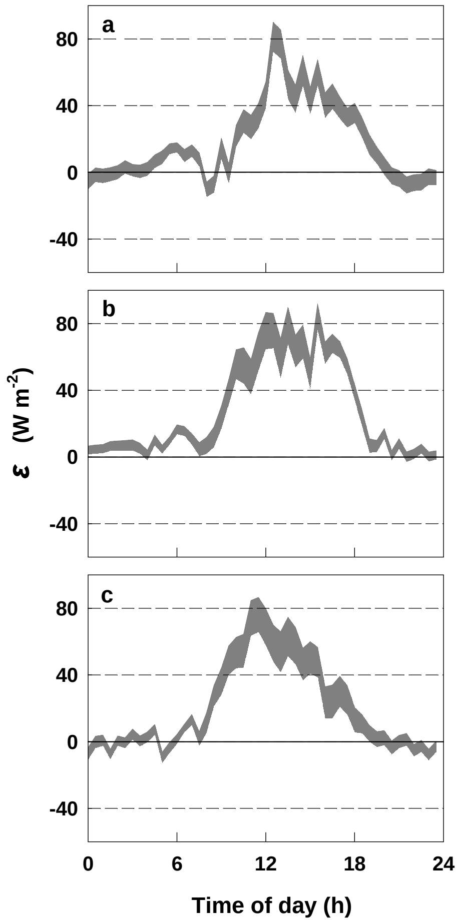

Fig. 1. Uncertainties in energy balance closure residuals (ε) due to spatial variability in R_n. The upper and lower bounds of the gray band derived from the maximum and minimum R_n of the eight treatments, respectively. Site I, a, II, b, III, c. Data are derived from Experiment 1.

BGD
8, 2001–2033, 2011

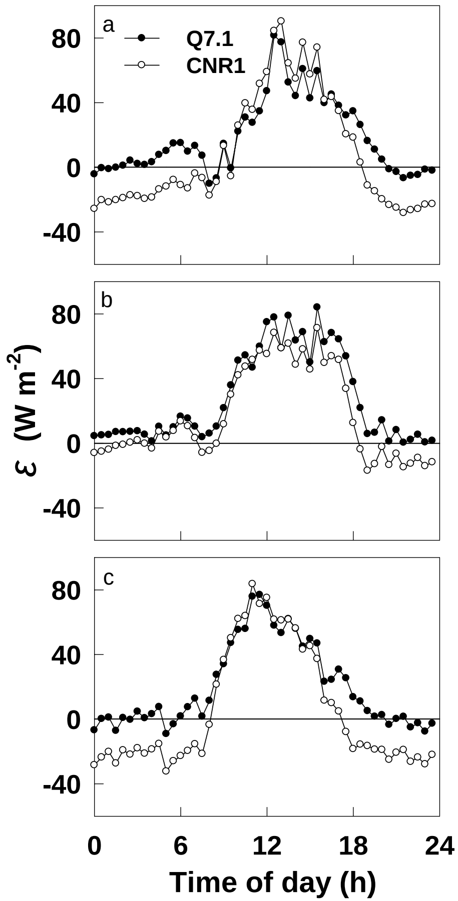

Fig. 2. Energy balance closure residuals (ε) derived from Q7.1 and CNR1 measurements in R_n. Site I, a, II, b, III, c. Data are derived from Experiment 1. 30 min averages data from 12, 16 and 17 days at sites I, II and III, respectively, were compiled into one-day scale, the same as Fig. 1.

BGD

8, 2001–2033, 2011

Net radiation with energy balance closure

C. Shao et al.

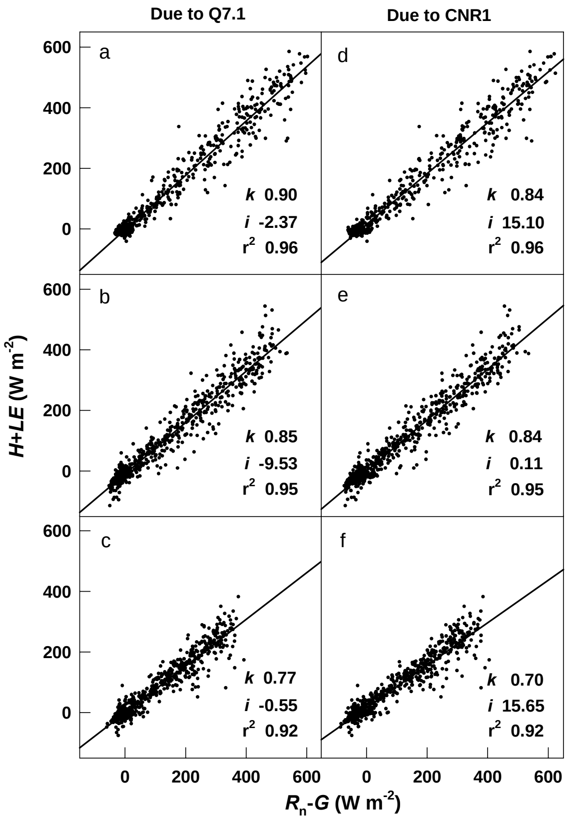

Fig. 3. Comparisons of 30 min values of turbulent ($H+\mathrm{LE}$) vs. available energy (R_n-G) derived from Q7.1 "(Left)" and CNR1 "(Right)" determined R_n with the ordinary least square (OLS) linear regression equation of $(H+\mathrm{LE})=k(R_n-G)+i$ (k, slope, i intercept, coefficient of determination, r^2 are also shown). The solid line shows OLS linear regression fit. Site I, "a, d"; II, "b, e"; III, "c, f". Data are derived from Experiment 1.

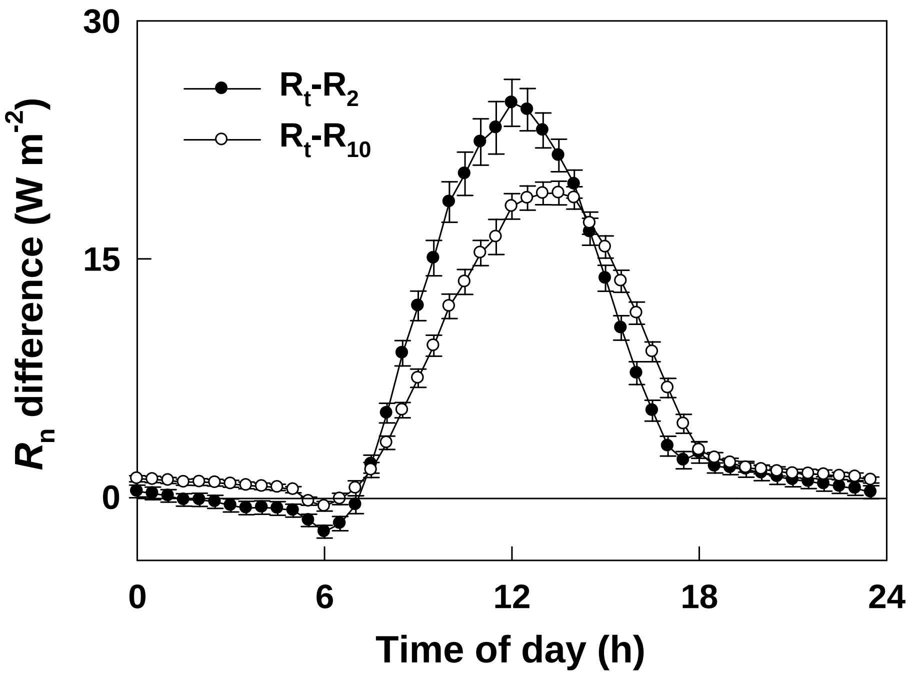

Fig. 4. Half-hourly differences of R_n between unclipped control and shoot clipped at 0.02 m ($R_t - R_2$) and at 0.10 m ($R_t - R_{10}$). Each value is the average of growing season from 3 June to 31 October 2007. Data are derived from Experiment 2.

BGD

8, 2001–2033, 2011

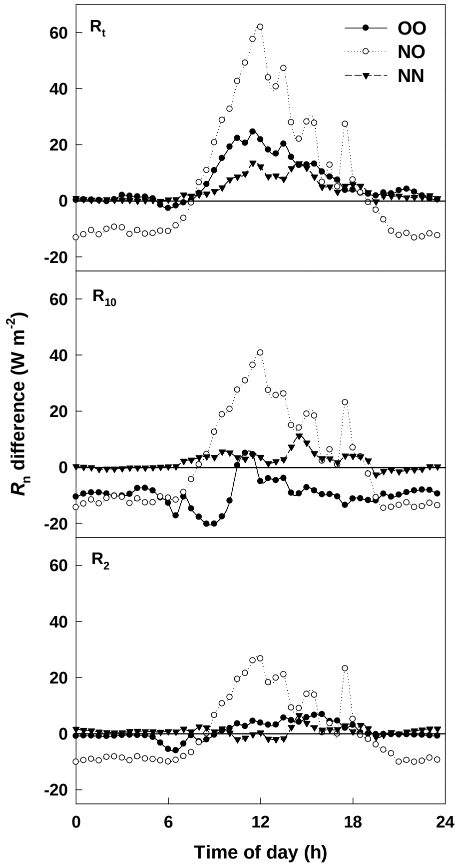

Fig. 5. R_n measurement results with Q7.1 affected by dome under new and old conditions. OO refers to the R_n result difference between two old domes, NO between new one and old one and NN between two new domes. R_t, R_{10} and R_2 refer to unclipped areas and areas with shoots clipped at 0.10 and 0.02 m at the end of each growing season, respectively. Data are derived from Experiment 3.

BGD
8, 2001–2033, 2011

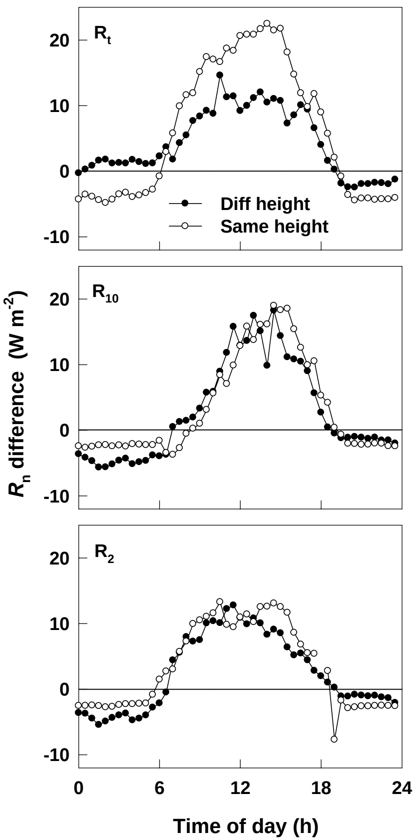

Fig. 6. Net radiometer deployment heights vs. R_n results (half-hourly data integrated into a diurnal scale). Diff height means R_n differences between the two Q7.1s deployed above the canopy by 0.5 and 1.5 m, respectively. Same height means both of the two Q7.1s deployed above the canopy by 0.5 m. R_t, R_{10} and R_2 see Fig. 5. Data are derived from Experiment 4.

BGD
8, 2001–2033, 2011